

# Electrical properties of PZT thin films grown by sol–gel and PLD using a seed layer

S.K. Pandey<sup>a,\*</sup>, A.R. James<sup>a</sup>, Chandra Prakash<sup>a</sup>, T.C. Goel<sup>b</sup>, K. Zimik<sup>c</sup>

<sup>a</sup>*Solid State Physics Laboratory, Lucknow Road, Timarpur, Delhi 110054, India*

<sup>b</sup>*Department of Physics, Indian Institute of Technology, New Delhi 110016, India*

<sup>c</sup>*Laser Science and Technology Centre, Metcalfe House, Delhi 110054, India*

Received 7 June 2004; accepted 23 June 2004

## Abstract

Lead Zirconate Titanate (PZT) thin films (with molar ratio of Zr:Ti::65/35) were deposited by pulsed laser deposition (PLD) and sol–gel technique on Pt/Si (1 1 1), and Pt/Si (1 0 0) substrates. A seed layer of PbTiO<sub>3</sub> (0.1 μm) was coated by sol–gel on the substrates before depositing PZT by PLD and sol–gel. A metal/ferroelectric/metal (MFM) capacitor structure, formed by depositing gold electrode on top of the film, was used for *C–V* and *P–E* measurements. A large remnant polarization ( $P_r = 56.8 \mu\text{C}/\text{cm}^2$ ) was observed on Pt/Si (1 1 1) substrates for the films deposited by sol–gel. Comparison of properties of PZT film deposited by these two techniques is discussed.

© 2004 Elsevier B.V. All rights reserved.

**Keywords:** Ceramics; Thin films; Electrical measurements; Oxides, Zirconium

## 1. Introduction

PZT thin films have been of great interest for many years for their applications in electronic devices, such as non-volatile memories, infrared sensors, optical shutters, electro-optic device modulators, actuators, multilayered capacitors (MLCs), etc. [1–3]. In the last few years perovskite structured ferroelectric thin films have been given a lot of attention due to the possibility of replacing current CMOS memory used for Random Access Memories with non-volatile Ferroelectric Random Access Memories (FRAM). Low-density FRAMs have been available commercially for several years, but the aim is high density FRAMs that are now being developed. For memory applications, the requirements include high remnant polarization ( $P_r$ ), low coercive field ( $E_c$ ) allowing operation at low voltages, good square hysteresis loops, short switching times, good retention, and fatigue properties. Internal electric fields developed by charged defects near the electrodes or in the film volume

are believed to play an important role in these phenomena [4–5]. Thus, correlated polarization–electric field (*P–E*) and capacitance–voltage (*C–V*) measurements are necessary in order to reveal the presence of space-charge regions (SCR) and to elucidate the problem of conduction mechanisms in PZT thin films [6].

A variety of techniques have been proposed to fabricate PZT films, such as metallorganic chemical vapor deposition (MOCVD), sputtering, sol–gel and PLD. Among them the sol–gel technique is the most popular because of its low cost and ease of fabrication for the PZT system [7]. However, PLD is popular for its ease of reproduction of stoichiometric PZT thin films [8].

In this article, we report on the structural and electrical properties of sol–gel and PLD grown Pb(Zr<sub>0.65</sub>Ti<sub>0.35</sub>)O<sub>3</sub> films. This composition lies in the rhombohedral part of the PbZrO<sub>3</sub>–PbTiO<sub>3</sub> phase diagram and has been recognized as a potential material for ferroelectric and electro-optic applications in the thin film form. All the films grown in this study had a seed layer of PbTiO<sub>3</sub> (deposited by sol–gel). The usage of a seed layer has been shown to be beneficial by several workers [3,9].

\* Corresponding author. Tel.: +91 11 23921692; fax: +91 11 23913609.  
E-mail address: 628@ssplnet.org (S.K.Pandey).

## 2. Experimental details

### 2.1. Deposition of films using sol–gel technique

The sol–gel PZT thin films were prepared using lead acetate tri-hydrate, zirconium-acetyl-acetonate, and titanium-isopropoxide as precursors. 2-Methoxy-ethanol and acetic acid were used as solvents. The molar ratio of Zr/Ti was 65/35 and a 4% excess of the lead precursor was added to the solution to compensate for the deficiency in lead concentration and to assist crystallization. Pt/TiO<sub>2</sub>/SiO<sub>2</sub>/Si (1 1 1) and Pt/TiO<sub>2</sub>/SiO<sub>2</sub>/Si (1 0 0) were used as substrates. Seed layers of PbTiO<sub>3</sub> were deposited by sol–gel technique using above-mentioned alkoxides (~0.1 μm thickness). A spin coating unit was used for the deposition of all sol–gel films. Substrates held by a vacuum-chuck were rotated at speeds of 2000 rpm for 20 s each. These films were pyrolysed intermediately at ~200 °C for 2 min, twice and finally at 600 °C. The seed layer was coated on all substrates prior to deposition of the PZT layers. The procedure followed for pyrolysis of PZT films was the same as the one in the case of the PT seed layers. After coating the PZT layer, the final crystallization was achieved by annealing at 650 °C, for 120 min in air. The metal/ferroelectric/metal (MFM) structure was formed by depositing gold top electrodes using cold dc sputtering (Model no. Denton Vacuum Sputter Coater—350) ~500 μm in diameter using a physical mask. It is to be noted that the structure is asymmetric in terms of electrodes, the bottom being platinum and the top electrode gold. It has been reported that an interfacial layer could form at the interface with Pt electrode during crystallization annealing, altering the properties of the PZT film [10,11]. The details about the technique have also been reported [12].

### 2.2. Deposition of films using PLD technique

A Pb(Zr<sub>0.65</sub>Ti<sub>0.35</sub>)O<sub>3</sub> target with 40 wt.% excess PbO was prepared by the solid state reaction technique in which a conventional sintering process was used. AR grade PbO, ZrO<sub>2</sub> and TiO<sub>2</sub> powders were used as starting materials. These oxides were mixed in appropriate proportions, ball milled, dried and then calcined at 800 °C and 850 °C, respectively, for 4 h. The resulting calcined powder was uniaxially pelletised using a hydraulic press at a pressure of 10 kN/m<sup>2</sup> and sintered at 1250 °C for 4 h in a lead-rich atmosphere. This resulted in a dense target, whose surface was polished for use in the PLD chamber. The conditions for deposition of thin films by PLD are given in Table 1.

### 2.3. Characterisation

The thickness of the films was estimated using a Dektak-3 stylus profilometer. In this case chemical etching of the thin films created a physical step. The morphology of the films was characterized using atomic force microscopy (AFM, NT-MDT Solver P47H) in the resonant mode. The interfaces

Table 1

Deposition parameters for PZT thin film (by PLD)

Substrate	Pt/TiO <sub>2</sub> /SiO <sub>2</sub> /Si
Target	Pb (Zr <sub>0.65</sub> Ti <sub>0.35</sub> )O <sub>3</sub> ceramic disc (with 40 wt.% excess PbO)
Target diameter	1 in.
Substrate target distance	~5 cm
Substrate (heater) temperature	250 °C
Base vacuum	~3 × 10 <sup>-6</sup> Torr
O <sub>2</sub> pressure	~100 × 10 <sup>-3</sup> Torr
Laser source	KrF Excimer, 650 mJ, 25 ns, 10 Hz
Laser energy used	250 mJ/pulse
Repetition rate	5 Hz
Deposition time	40 min
Energy fluence	~1.5 J/cm <sup>2</sup>
Post-deposition ex situ anneal	650 °C/2 h

were studied by scanning electron microscopy (SEM, Model No. LEO-1430). XRD patterns were recorded on a Philips thin film diffractometer (Model PW 3020) using a Cu Kα 1.54 Å X-ray in parallel beam geometry. The incident X-ray beam made an angle of 1.5° with the sample. A graphite monochromator was used in the secondary optics to minimize the background fluorescence/scattering.

Hysteresis loops were recorded using an automatic *P–E* loop tracer (RT-66A) of Radiant Technologies Inc. The remnant polarization (*P<sub>r</sub>*) and coercive field (*E<sub>c</sub>*) were obtained from the *P–E* hysteresis loop. Measurements were done on several dots of the films also on different films at several different voltages.

*C–V* measurements were done using an HP-4294A Impedance Analyser at 100 kHz with an oscillator level of 100 mV and a delay of 2 s.

## 3. Results and discussion

An X-ray diffractogram showing patterns of PZT (65/35) bulk and thin films deposited by laser ablation and sol–gel techniques is given in Fig. 1. The XRD pattern shows the

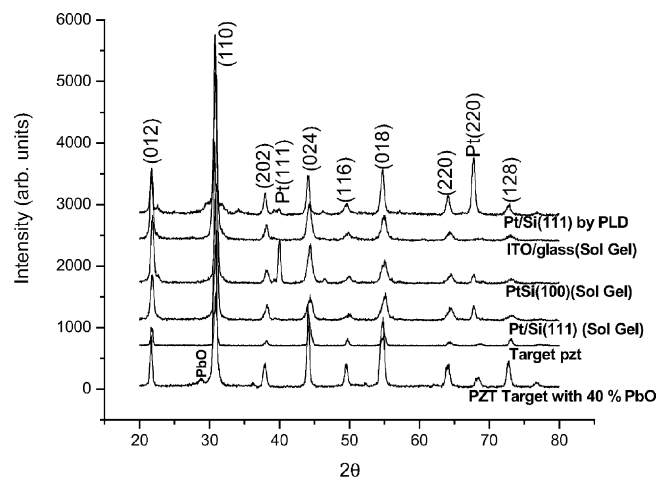


Fig. 1. X-ray diffractogram of PZT thin films deposited by sol–gel and PLD.

formation of a single-phase perovskite for PZT bulk and thin films. Formation of the un-wanted pyrochlore phase was eliminated through a careful selection of deposition parameters. The films deposited were polycrystalline in nature. PZT films grown by PLD and sol-gel were all  $\sim 0.5 \mu\text{m}$  thick. The SEM micrograph (Fig. 2) clearly reveals the surface morphology of the PZT layer. However, the interface between Pt and PZT is clean with no trace of any inter diffusion. This strongly suggests that the intermediate PT layer in addition to serving as a seed layer acts as a barrier, preventing the inter-diffusion of PZT into the substrate.

The underlying PT layer would also obviously have to be considered in so far as its effects on the (enhanced)  $P_r$  values of the films deposited. The exact band structure would have to be arrived at in order to ascertain the contributions of this layer and its effect on the overall properties of the films. As a first thought, it would appear prudent to imagine that the PT layer serves as a barrier to prevent diffusion of PZT into the substrate as opposed to frequently observed diffusion phenomena in films which have no such buffer layers. This could be on account of the fact that the interface is extremely smooth, allowing for very precise switching characteristics of the buffered PZT thin films.

The strains in a thin film have always been the matter of considerable concern, on account of the fact that the properties of the films are greatly dependent upon the effects of strain in them. Although the strains in these films have not been studied in this research, it is felt that the strain in these polycrystalline films may be relatively lower. This is because a polycrystalline system provides for alleviation of stress through relaxation mechanisms, generally found to occur much more slowly in epitaxial films.

### 3.1. AFM measurements

The AFM micrographs are shown in Fig. 3a–c. The average surface roughness ( $R_a$ ) in PZT films deposited on

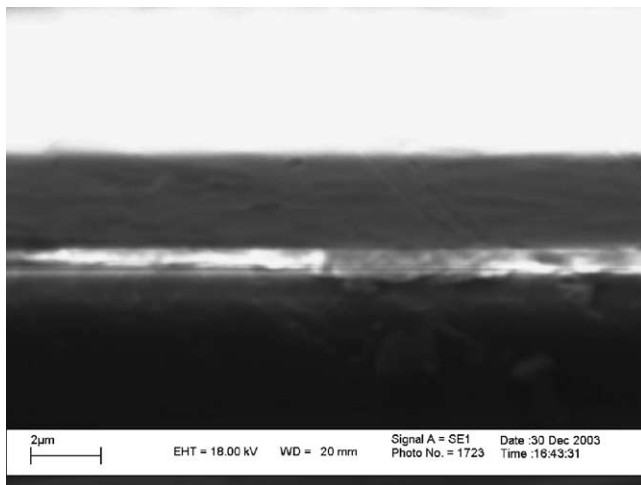
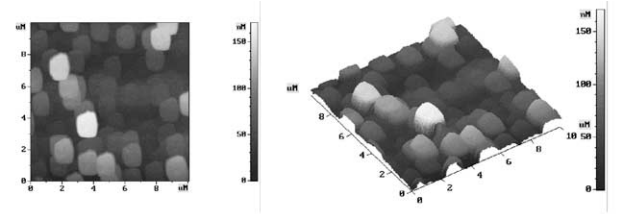
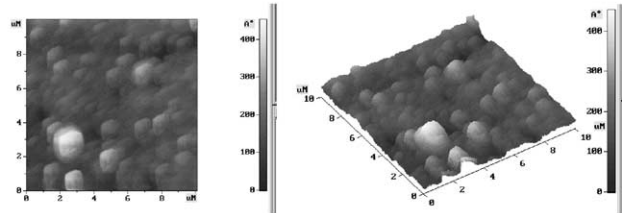


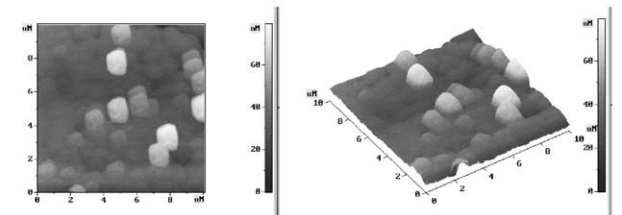
Fig. 2. SEM micrograph of PZT thin film deposited by sol-gel on Pt/Si (1 1 1).



(a) PZT/PT/Pt/TiO<sub>2</sub>/SiO<sub>2</sub>/Si(111) by PLD



(b) PZT/PT/Pt/TiO<sub>2</sub>/SiO<sub>2</sub>/Si(100) by Sol Gel



(c) PZT/PT/Pt/TiO<sub>2</sub>/SiO<sub>2</sub>/Si(111) by Sol Gel

Fig. 3. Atomic force micrographs (plane and 3-D views): (a) PZT/PT/Pt/TiO<sub>2</sub>/SiO<sub>2</sub>/Si (1 1 1) by PLD, (b) PZT/PT/Pt/TiO<sub>2</sub>/SiO<sub>2</sub>/Si (1 0 0) by sol-gel, (c) PZT/PT/Pt/TiO<sub>2</sub>/SiO<sub>2</sub>/Si (1 1 1) by sol-gel.

Pt/Si (1 1 1) by sol-gel is 0.7 nm. The growth in the film also looked oriented. The PZT films deposited by sol-gel on Pt/Si (1 0 0) substrates have a surface roughness of 3.832 nm and by PLD on Pt/Si (1 1 1) is 24.243 nm. Hence it is evident from the fact that the increase in polarization is due to smooth nanosize surface roughness.

### 3.2. $P$ – $E$ measurements

Table 2 shows the values of remnant polarization and coercive field for all the films grown in this study. The  $P_r$  values found in some of our films are relatively higher than even bulk values. This may be ascribed to the optimization of synthesis conditions, through which a very fine interface was formed in between each layer. It is well known that a good interface is detrimental to obtaining a high quality film, thereby resulting in enhanced electrical property output. It maybe noted that a lot of research has been done to improve the quality of the interface between PZT and underlying buffer layers/substrates and it has been found that the fatigue in films with good interfacial morphology is greatly alleviated, making them fatigue resistant [8]. The value of  $P_r$  in the PZT/PT/Pt/Si (1 1 1) films deposited by the sol-gel technique was found to be  $56.8 \mu\text{C}/\text{cm}^2$ , as shown in Fig. 4 and is better than the values reported for the same composition by Tyunina et al. [13] and Boerasu et al. [6].

Table 2

Remnant polarisation and coercive field of PZT thin films grown by different techniques

Substrates	Technique	Remnant polarisation ( $P_r$ ) ( $\mu\text{C}/\text{cm}^2$ )	Coercive field ( $E_c$ ) (kV/cm)
Pt/TiO <sub>2</sub> /SiO <sub>2</sub> /Si (1 1 1)	PLD	19.6	60.2
Pt/TiO <sub>2</sub> /SiO <sub>2</sub> /Si (1 0 0)	Sol-gel	36.8	71.9
Pt/TiO <sub>2</sub> /SiO <sub>2</sub> /Si (1 1 1)	Sol-gel	56.8	51.1

Tyunina et al. reported values of  $P_r$  and  $E_c$  as  $17 \mu\text{C}/\text{cm}^2$  and  $50 \text{ kV}/\text{cm}$ , respectively. However, Boerasu et al. reported values of  $P_r$  and  $E_c$  as  $9 \mu\text{C}/\text{cm}^2$  and  $39 \text{ kV}/\text{cm}$ , respectively, by sol-gel. The improvement in the ferroelectric properties in terms of higher  $P_r$  may perhaps be related to the fact that the films in this study have a larger grain size ( $\sim 1 \mu\text{m}$ ) compared to the films deposited by a XeCl excimer laser ( $\lambda = 308 \text{ nm}$ ) in which the maximum grain size of the films observed was  $0.1 \mu\text{m}$  [13]. A higher  $P_r$  of  $30 \mu\text{C}/\text{cm}^2$  for higher grain size was reported by Lee et al. [14] on account of the larger grain size of the films. A remnant polarization ( $P_r$ ) of  $13 \mu\text{C}/\text{cm}^2$  (for randomly oriented films) and  $23 \mu\text{C}/\text{cm}^2$  (for films with preferred orientations) was reported by Kang et al. [3]. Thus, the nanosize smooth surface and oriented growth of the films are the main reasons for higher remnant polarization ( $P_r$ ). Although from the X-ray data taken on our films, there does not seem to be any particular orientation or texture, the values of  $P_r$  seem to be very high. It is well known that the magnitude of polarization is not only affected by the clamping of the film by the substrate, but also by domain structure as well as the mobility of the domain walls. For the rhombohedral structure, if one considers possible orientations of domains for the two crystallographic orientations, two types of domains exist in the (1 1 1)-oriented films. There is one possible orientation normal to the film surface and three canted an angle of approximately  $71^\circ$  or  $109^\circ$  with the normal to the film. As

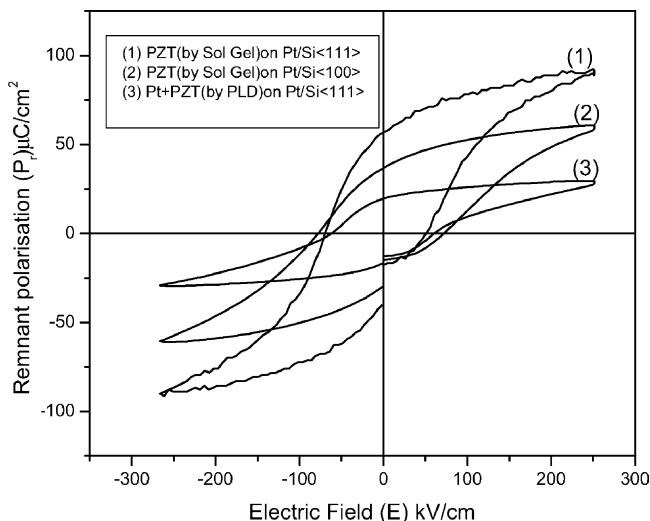


Fig. 4. Polarisation vs. electric field hysteresis loops.

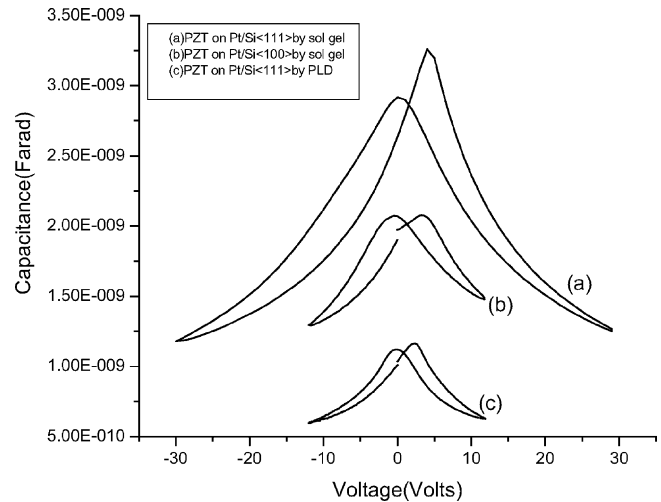


Fig. 5. Capacitance vs. voltage curves.

the polarization is switched from one type to the other by an electric field, the reorientation is accompanied with strain.

A cursory look at the hysteresis loop shown in Fig. 4 shows a well-defined curve, indicative of the absence of any pinning effects on domain boundary motion on account of defects.

### 3.3. $C$ - $V$ measurements

The  $C$ - $V$  curves for the films are shown in Fig. 5. All curves have the typical butterfly shape with two maxima that should correspond to the coercive fields. The values of voltages obtained from the two maxima of the  $C$ - $V$  curve divided by thickness of the film should be equal to twice the coercive field ( $E_c$ ) of the  $P$ - $E$  curve. In this case both the values are comparable. A difference in the value may be attributed to space charge regions, which could develop due to dc biasing in the  $C$ - $V$  measurements.

## 4. Conclusions

Single-phase PZT thin films were deposited on various substrates by sol-gel and PLD (using a KrF excimer laser on Pt/Si (1 1 1)) techniques using a seed layer of lead titanate ( $\text{PbTiO}_3$ ) and the electrical properties have been compared. The AFM picture shows good surface morphology having nanosize surface roughness and a grain size of  $\sim 1 \mu\text{m}$  for the PZT films. A high value of remnant polarization ( $P_r$ ) has been obtained for the films deposited on Pt/Si (1 1 1) substrates by sol-gel technique.

## Acknowledgements

The authors wish to thank D.S. Rawal and Anshu Goyal for their help in recording SEM micrographs and XRO patterns.

## References

- [1] J.F. Scott, L. Kammerdimer, M. Parris, S. Trayner, V. Ottenbacher, A. Shawabke, W.F. Oliver, *J. Appl. Phys.* 64 (1988) 787.
- [2] M. Okuyama, Y. Matsui, H. Nakamo, Y. Hamakawa, *Ferroelectrics* 33 (1981) 235.
- [3] H.S. Kang, W.J. Lee, *J. Vac. Sci. Technol. A* 20 (4) (2002) 1498.
- [4] U. Robels, J.H. Calderwood, G. Arlt, *J. Appl. Phys.* 77 (1995) 4002.
- [5] M. Grossman, O. Lohse, D. Bolten, U. Boettger, T. Schneller, R. Waser, *J. Appl. Phys.* 92 (2002) 2680.
- [6] I. Boerasu, L. Pintilie, M. Pereira, M.I. Vasilevskiy, M.J.M. Gomes, *J. Appl. Phys.* 93 (2003) 4776.
- [7] G. Yi, Z. Wu, M. Sayer, *J. Appl. Phys.* 64 (1988) 2717.
- [8] O. Auciello, R. Dat, R. Ramesh, in: Carlos, P. de Araujo, J.F. Scott, G.W. Taylor (eds.), *Ferroelectric Thin Films: Synthesis and Basic Properties*, 525 pp.
- [9] H. Du, D.W. Johnson Jr., W. Zhu, J.E. Grabner, G.W. Kammlot, S. Jin, J. Rogers, R. Willett, R.M. Fleming, *J. Appl. Phys.* 86 (4) (1999) 2220.
- [10] S. Chung, J.W. Kim, G.H. Kim, C.O. Park, W.J. Lee, *Jpn. J. Appl. Phys. Part 1* 36 (1997) 4386.
- [11] Z. Huang, Q. Zhang, R.W. Whatmore, *J. Appl. Phys.* 86 (1999) 1662.
- [12] M. Es Souni, M. Abed, C.H. Solterbeck, A. Piorra, *Mater. Sci. Eng. B* 94 (2002) 229.
- [13] M. Tyunina, J. Levoska, A. Sternberg, S. Leppavuori, *J. Appl. Phys.* 84 (1998) 6800.
- [14] J.-S. Lee, E.-C. Park, J.-H. Park, B.-I. Lee, S.-K. Joo, *Ferroelectric Thin Films VIII*, in: *Mater. Res. Soc. Symp. Proc.*, vol. 596, p. 217.